Gelatin methacryloyl hydrogel scaffold loaded with activated Schwann cells attenuates apoptosis and promotes functional recovery following spinal cord injury

YANG LIU[1,2*], HAO YU[1,2*], PENG YU[1,2*], PENG PENG[1,2], CHAO LI[1,2], ZHENYANG XIANG[1,2] and DEXIANG BAN[1,2]

[1]Department of Orthopedics, Tianjin Medical University General Hospital; [2]International Science and Technology Cooperation Base of Spinal Cord Injury, Tianjin Key Laboratory of Spine and Spinal Cord Injury, Department of Orthopedics, Tianjin Medical University General Hospital, Heping, Tianjin 300052, P.R. China

Received May 25, 2022; Accepted October 21, 2022

DOI: 10.3892/etm.2023.11843

Abstract. Spinal cord injury (SCI) is a refractory disease of the central nervous system with a high disability and incidence rate. In recent years, bioactive material combined with cell transplantation has been considered an effective method for the treatment of SCI. The present study encapsulated activated Schwann cells (ASCs) in a 3D gelatin methacryloyl (GelMA) hydrogel in order to investigate its therapeutic effects on SCI. ASCs were isolated from previously ligated rat sciatic nerves. Scanning electron microscopy and live/dead staining were used to evaluate the biocompatibility of hydrogels with the ASCs. The scaffold was transplanted into the spinal cord of rats in the hemisection model. Behavioral tests and hematoxylin and eosin staining were employed to assess the locomotion recovery and lesion areas before and after treatment. Cell apoptosis was evaluated using TUNEL staining and immunochemistry, and apoptosis-related protein expression was detected using western blot analysis. The ASCs exhibited a favorable survival and proliferative ability in the 3D GelMA hydrogel. The scaffold transplantation significantly reduced the cavities and improved functional recovery. Moreover, the GelMA/ASCs implants significantly inhibited cell apoptosis following SCI and this effect may be mediated via the p38 MAPK pathway. Overall, these findings indicated that ASCs combined with the 3D GelMA hydrogel may be a promising therapeutic strategy for SCI.

Correspondence to: Professor Dexiang Ban, Department of Orthopedics, Tianjin Medical University General Hospital, 154 Anshan Road, Heping, Tianjin 300052, P.R. China
E-mail: dxbantmu@163.com

*Contributed equally

Key words: gelatin methacryloyl hydrogel, Schwann cells, biomaterials, scaffold, spinal cord injury, cell apoptosis, function recovery

Introduction

Spinal cord injury (SCI) is a highly debilitating neurological trauma caused by traumatic injury or disease (1). The induced damage causes a series of pathological changes, including hemorrhage, inflammation, edema and fibrous scar formation, markedly impair neuron regeneration and functional recovery following SCI. Moreover, the self-recovery capacity of the central nervous system is inherently poor (2,3). Thus, majority of patients with SCI suffer from lifelong disabilities. Thus, its clinical treatment remains a worldwide challenge (4).

Previous studies using rodent models have demonstrated that cell transplantation is a promising repair strategy for SCI. Generally, the transplanted healthy cells can replace damaged cells, and simultaneously secrete a variety of neurotrophic factors required for axon remyelination and neuronal regeneration (5,6). However, directly injecting the cell suspension into the cavities usually cannot achieve ideal therapeutic efficacy. A vast number of cells are lost during the injection and the harsh microenvironment of the injured spinal cord contributes to the necrosis or apoptosis of 80% of the transplanted cells (7,8). Co-transplantation with a biocompatible scaffold provides available solutions for this issue. The seed cells are encapsulated in the scaffold and the scaffold creates a suitable local environment to enhance cell retention and the survival rate (9-11). Currently, the combination of biomaterial with cell transplantation is under intense investigation in the scope of SCI.

Schwann cells (SCs) are glial cells in the peripheral nervous system. They play a notable role in Wallerian degeneration and the regeneration of the injured peripheral nerve (12,13). Following peripheral nerve injury, the resting SCs are activated, proliferate and migrate to the injury site, and co-phagocytose damaged axonal myelin with macrophages. Furthermore, activated SCs (ASCs) secrete numerous nutritional factors, cell-adhesion molecules and extracellular matrix (ECM) to promote and guide neuronal regeneration (14). In SCI research, SC transplantation therapy has exhibited immense potential. Accumulating evidence has indicated that the transplantation of SCs inhibits inflammation, reduces cyst formation and promotes axon elongation. In addition, motor and functional

recovery have also been observed (15,16). SCs are considered promising candidate cells for SCI repair. However, single SC therapy is also associated with difficulties as aforementioned.

Gelatin methacryloyl (GelMA) hydrogel is a photosensitive hydrogel. It is mainly processed from the native ECM which confers its favorable biocompatibility (17). Furthermore, GelMA hydrogel possesses highly adjustable physiochemical properties and an inner three-dimensional structure, which render it an effective option as a vehicle for cell delivery (18,19). To date, certain researchers have co-transplanted GelMA hydrogels with various cells to repair the injured spinal cord, including bone marrow-derived mesenchymal cells (BMSC), neural stem cells (NSC) and induced pluripotent stem cells (iPSCs), and the results have been satisfactory (20,21). However, the therapeutic efficacy of ASC-loaded GelMA hydrogel for SCI has not yet been evaluated, at least to the best of our knowledge.

The present study transplanted ASC-loaded GelMA hydrogels into rat spinal-transected segments. Through behavioral and histological analyses, the present study aimed to evaluate the therapeutic efficacy of ASC-loaded GelMA hydrogel in SCI repair.

Materials and methods

Ethics. Sprague-Dawley (SD) female rats (8-weeks old, 180-250 g body weight) used in this experiment were obtained from SPF (Beijing) Biotechnology Co., Ltd. [permission number: SCX (JING) 2019-0010]. The rats were group-housed 2-3 per cage and maintained with a 12-h light/dark cycle (light at 7 a.m.) under a temperature (22-23˚C) and humidity (55-65%)-controlled environment. They were given free access to food and water and acclimated for at least 7 days before the surgery for the adaption to the environment. All procedures involving animals complied with the Guiding Principles for the Care and Use of Vertebrate Animals in Research and Training. The experiments were approved (approval no. MDL20210810-01) by the Animal Ethical and Welfare Committee of The Tianjin Medical University General Hospital (Tianjin, China).

Isolation and identification of ASCs. The isolation, culture and identification of ASCs have been previously described (22). Briefly, an 8-week-old SD rat was anesthetized with an intraperitoneal injection of pentobarbital sodium (30 mg/kg). To change SCs into ASCs, following anesthesia, the bilateral sciatic nerves were ligated for one week. Then the rat was sacrificed with intraperitoneal injection of excess pentobarbital (300 mg/kg) and the bilateral sciatic nerves distal to the ligation spot were isolated. After removing the endoneurium, the remaining nerve tissues were cut into 0.5-1 mm^3 fragments. The nerve tissues were digested with 0.05% collagenase (cat. no. C8176; MilliporeSigma) for 45 min at 37˚C and subsequently replaced with culture medium comprised of Dulbecco's modified Eagle's medium (DMEM; cat. no. C11330500BT; Gibco; Thermo Fisher Scientific, Inc.) and 10% fetal bovine serum (FBS; cat. no. 10100147; Gibco; Thermo Fisher Scientific, Inc.). The mixture was transferred to a 15-ml centrifuge tube. Following centrifugation (200 x g, 4˚C, 5 min), the supernatant was discarded and the sediment was resuspended with DMEM supplemented with 10% FBS and 1% antibiotic solution (penicillin, streptomycin) (cat. no. 15070063; Gibco; Thermo Fisher Scientific, Inc.). The cell suspension was placed into a 25-ml culture flask and incubated at 37˚C and 5% CO_2. The culture medium was changed every 3 days. After 1 week, the ASCs reached a confluency of 90% and the identity was confirmed by immunostaining of S-100 (1:250; cat. no. ab109384; Abcam). After nuclei staining with 5 μg/ml DAPI for 10 mi at room temperature, cells were observed under a fluorescence inverted phase contrast microscope (Olympus Corporation).

Preparation and evaluation of ASC-GelMA hydrogels. The freeze-dried GelMA powder was purchased from MilliporeSigma. The hydrogel was obtained by dissolving 3% (W/V) lyophilized powder and 0.5% (W/V) lithium phenyl-2,4,6-trimethylbenzoylphosphinate (LAP) into phosphate-buffered saline (PBS), followed by exposure to 405 nm UV irradiation for 15 sec.

The ASCs were trypsinized, centrifuged (200 x g, 4˚C, 5 min), and then resuspended in 3% (w/v) GelMA solution at the concentration of $1x10^7$/ml. Under the exposure of 405 nm UV irradiation for 15 sec, the cell-seeded GelMA hydrogel was obtained. The hydrogel was then transferred into a six-well plate in which ASC basal medium was added followed by culture at 37˚C with 5% CO_2. Because the gel reflected the light and ASCs were encapsulated in the gels, the cells could be hardly observed under the light microscope. Scanning electron microscopy (SEM, S-3400; Hitachi, Ltd.) was then used to observe the microstructure of the GelMA hydrogel with or without seeded cells. After 1, 3 and 5 days of *in vitro* culture, the biocompatibility of the GelMA hydrogel with ASCs was evaluated using Calcein-AM/ethidium staining according to the manufacturer's procedure (cat. no. BL3224; Invitrogen; Thermo Fisher Scientific, Inc.).

Animal experiments

Design and spinal cord surgery. A total of 80 SD rats were used in the experiments and they were randomly divided into four groups as follows: The sham group (n=20), the SCI group (n=20), the ASC group (n=20) and the GelMA/ASC group (n=20).

Spinal cord hemi-transection and scaffold transplantation. Firstly, the healthy adult SD rats were deeply anesthetized with an intraperitoneal injection of pentobarbital (30 mg/kg). With the back shaved and the skin disinfected, a midline incision over the spinous process of ~2 cm was made to expose T9-T11. The paravertebral muscles and the surrounding connective tissue were also cut using micro scissors. The T9-T10 laminectomy was performed. For the latter three groups (SCI, ASC and GelMA/ASC groups), the right lateral hemisection at T10 was performed to create a gap of ~2 mm in length. For the ASC group, the ASC suspension with a cell density of $1x10^7$/ml was injected; for the GelMA/ASCs group, the prepared cell-loaded scaffold was transplanted. The incision was then closed and the rat bladders were manually expressed twice a day until the urinary function recovered. Antibiotics (penicillin, 40,000 μ/kg/day) were also administered to prevent post-operative infection.

Behavioral assessment. The Basso-Beattie-Bresnahan (BBB) scoring system was used to evaluate hindlimb motor function. This is an open-field locomotor evaluation test scoring 21 points, with 0 indicating no movement of hindlimbs and 21 indicating normal levels (23). Prior to the evaluation, the rat was separately placed in an open field with a non-slippery surface and allowed to move freely for 5 min. Two independent observers blinded to the grouping of the rats scored the rat's motor performance according to the BBB scale. The test lasted 4 min and once the rat stopped moving for 1 min, it was placed in the center of the open field again for a re-test.

The inclined plate test was also used for a behavioral assessment. The rat was placed on a plate covered with a 6-mm-thick rubber pad. According to the previous study, the body axis of the rats was perpendicular to the orientation of the plate (24). The plate was then lifted 5˚ every 30 sec and the maximum degree at which the rat could maintain its balance was recorded. Each rat was tested three times and the mean value was the final angle for the individual rat. The behavioral tests were performed from week 1 to week 6 after surgery until all the rats were sacrificed.

Sample harvesting and histological analysis. At 7 and 42 days after surgery, 3 rats were randomly selected and deeply anesthetized with an intraperitoneal injection of pentobarbital (30 mg/kg). Following heart perfusion with 150 ml pre-cooled PBS containing 4% paraformaldehyde, ~10 mm spinal cord containing the injury site was dissected. It was then post-fixed overnight with 4% paraformaldehyde. The specimen was then embedded in paraffin and sliced into 5-μm-thick sections.

The samples collected at 42 days were stained with hematoxylin and eosin (H&E) to evaluate the lesion volume. Slices were stained with hematoxylin for 10 min and with eosin for 2 min at room temperature. The images were observed under an optical microscope and the volume was measured using ImageJ software (1.49 V; National Institutes of Health).

Terminal deoxynucleotidyl transferase dUTP nick-end labeling (TUNEL) staining and immunochemistry. TUNEL assay kit (cat. no. C1086; Beyotime Institute of Biotechnology) staining was used to evaluate the number of apoptotic cells. The paraffin-embedded sections were stained according to the instructions of the manufacturer. The TUNEL-positive cells with green fluorescence were observed under a fluorescence microscope and six fields of view for each section were randomly selected for subsequent calculation using ImageJ software.

The streptavidin-biotin-peroxidase-complex method was used to detect Bcl-2 expression using immunochemistry. The paraffin-embedded sections were sequentially subjected to standard dewaxing, hydration, antigen retrieval and rinsing, followed by incubation with endogenous peroxidase blockers for 10 min, and sealing in serum for 20 min. After discarding the serum, the primary antibody Bcl-2 (1:250; cat. no. ab196495; Abcam) was added followed by incubation for 24 h at 4˚C. The following day, the sections were rinsed and a horseradish peroxidase (HRP)-conjugated goat anti-rabbit secondary antibody (1:500; cat. no. ab6721; Abcam) was added, followed by incubation for 30 min at 37˚C. After rinsing thoroughly, the streptomycin-biotin-peroxidase solution was added in a dropwise manner, reacting with the specimen for 20 min followed by diaminobenzidine (DAB) color development. Finally, the nuclei were counterstained with hematoxylin for 2 min at room temperature. Images were observed under an optical microscope and the Bcl-2 positive cells were counted using ImageJ software.

Western blot analysis. The tissue samples collected at day 7 after surgery were minced using eye scissors on ice and homogenized in 300 μl lysis buffer (cat. no. ST505; Beyotime Institute of Biotechnology) for 30 min. Homogenates were then centrifuged at 15,000 x g for 10 min at 4˚C and the supernatant was collected to quantify the protein concentration using a bicinchoninic acid (BCA) kit (cat. no. A53225; Thermo Fisher Scientific, Inc.) as per the manufacturer's instructions. Subsequently, equal amounts of protein (40 μg per lane) were separated by SDS-PAGE (10% of acrylamide) gel electrophoresis and transferred onto PVDF membrane. The membrane was blocked with 5% bovine serum albumin (BSA; cat. no. 9998; Cell Signaling Technology, Inc.) for 2 h at room temperature and then incubated with primary antibodies at 4˚C overnight. The following day, after three rinses with PBS, the membranes were incubated with the HRP-conjugated goat anti-rabit (cat. no. 7074) and horse anti-mouse (cat. no. 7076) secondary antibodies (1:1,000; Cell Signaling Technology, Inc.) for 1 h at room temperature. The bands were visualized in an enhanced chemiluminescence system (ChemiDox XRS; Bio-Rad Laboratories, Inc.) and images of the target proteins were semi-quantified using ImageJ software. The primary antibodies used were as follows: Anti-Bcl-2 (1:1,000; cat. no. ab196495; Abcam), anti-caspase-3 (1:1,000; cat. no. ab32351; Abcam), anti-p38 (1:1,000; cat. no. 8690; Cell Signaling Technology, Inc.), anti-p-p38 (1:1,000; cat. no. 4511; Cell Signaling Technology, Inc.), anti-ERK1/2 (1:1,000; cat. no. 9194; Cell Signaling Technology, Inc.), anti-p-ERK1/2 (1:1,000; cat. no. 4370; Cell Signaling Technology, Inc.), anti-JNK1/2 (1:1,000; cat. no. 3708; Cell Signaling Technology, Inc.), anti-p-JNK1/2 (1:1,000, cat. no. 9255, Cell Signaling Technology, Inc.), and anti-GAPDH (1:1,000, cat. no. AF0006, Beyotime Institute of Biotechnology).

Statistical analysis. All statistical analyses were performed using GraphPad Prism 8 software (GraphPad Software, Inc.). The comparison among multiple groups was performed by one-way ANOVA followed by Tukey's post hoc test. Significant differences in BBB locomotion evaluation were determined by the Kruskal-Wallis test with Dunn's multiple comparison. The data are presented as the mean ± standard deviation (SD) or median (IQR). $P<0.05$ was considered to indicate a statistically significant difference.

Results

Culture and identification of ASCs. At 10 days post-isolation of the ASCs, the ASCs proliferated and covered the T75 culture flask (Fig. 1A). The isolated cells expressed strong red fluorescence of the S100 SC marker after immunostaining (Fig. 1C). A previous study has demonstrated that ASCs exhibit a greater proliferative and adhesive ability than normal SCs (NSCs) (24). Thus, ASCs were used in the following experiments.

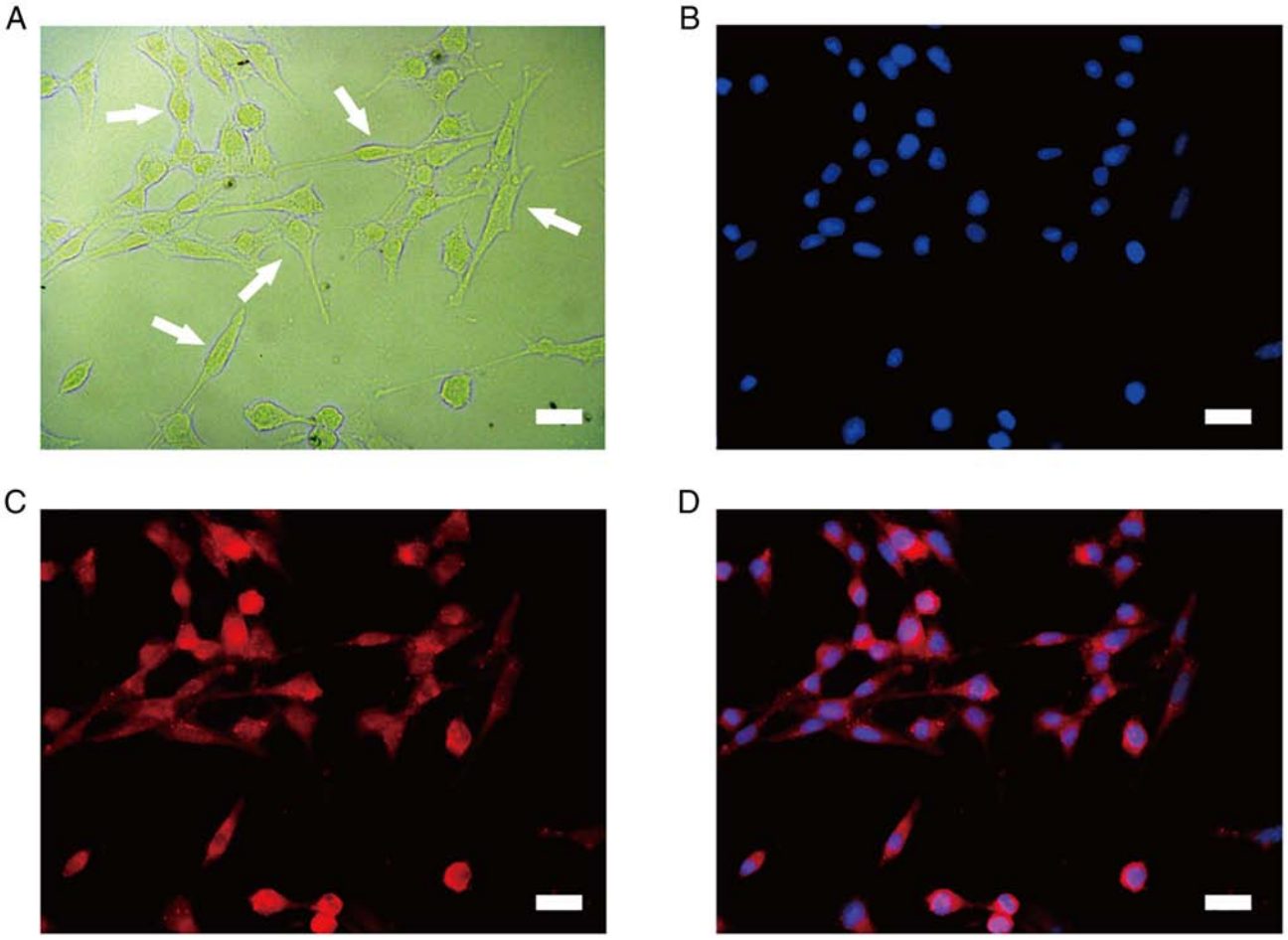

Figure 1. Characterization of rat ASCs. (A) Morphology of the ASCs under an optical microscope. Arrows indicate ASCs in the culture medium. (B) The nuclei of ASCs were stained with DAPI using immunofluorescence. (C) ASCs were marked with S-100 using immunofluorescence. (D) Schwann cells and nuclei of ASCs were merged using immunofluorescence. Scale bars, 25 μm. ASCs, activated Schwann cells.

Encapsulation of ASCs in GelMA hydrogel. The SEM results displayed the 3D porous microstructure of the GelMA hydrogel, which was essential for oxygen and nutrient exchange, as well as for promoting cell survival, proliferation and migration (Fig. 2A). Moreover, it was also found that the ASCs were well encapsulated in the GelMA hydrogel (Fig. 2B).

To further assess the viability of the ASCs encapsulated in the GelMA hydrogel, live/dead staining was performed. The green fluorescence indicated that the majority of encapsulated ASCs were alive and that the cells proliferated from days 1 to 5, as indicated by a gradual increase in green labels (Fig. 2C). Overall, the percentage of alive ASCs was >85% which indicated the favorable biocompatibility of the GelMA hydrogel (Fig. 2D).

Morphology of the lesion site, as revealed by H&E staining. Following 48 h of co-culture, the ASC-loaded GelMA hydrogel was transplanted into the hemisection area of the rat spinal cord (Fig. 3A). To determine whether the ASC-loaded GelMA hydrogel could repair the injured spinal cord, H&E staining was performed on the samples collected on day 42 following surgery (Fig. 3B). In the SCI group, H&E staining revealed large cavities and a disordered structure at the injury site. By contrast, the GelMA/ASC groups exhibited an evident decrease in volume and an improvement of tissue integrity ($P<0.01$). Moreover, compared with the ASC group, the cavities in the GelMA/ASC group were smaller, which demonstrated the improved tissue repair ability of ASCs when encapsulated in the GelMA hydrogel (Fig. 3C).

Evaluation of locomotor function. The ability of the ASC/GelMA hydrogel to repair SCI was also assessed by examining the recovery of hindlimb locomotor function. Thus, the BBB scoring system and inclined plate test were applied to evaluate the motor functional recovery of the rats with SCI from weeks 1 to 6 following surgery. Higher BBB scores or inclined angles represent an improved motor function and *vice versa*. In the beginning, the rats with SCI exhibited a significant decrease in both BBB scores and inclined angles, suggesting the loss of motor function following SCI. Subsequently, there were overall upward trends in both BBB scores and inclined angles for rats with SCI, suggesting the gradual recovery of their motor function. The GelMA/ASC groups presented significantly higher scores ($P<0.05$) and inclined angles ($P<0.01$) than the SCI group from 3 weeks post-injury onward up to the final evaluation (Fig. 4A and B). In particular, the GelMA/ASC group exhibited an improved therapeutic efficacy than single ASC treatment from the second week after surgery to the time of sacrifice.

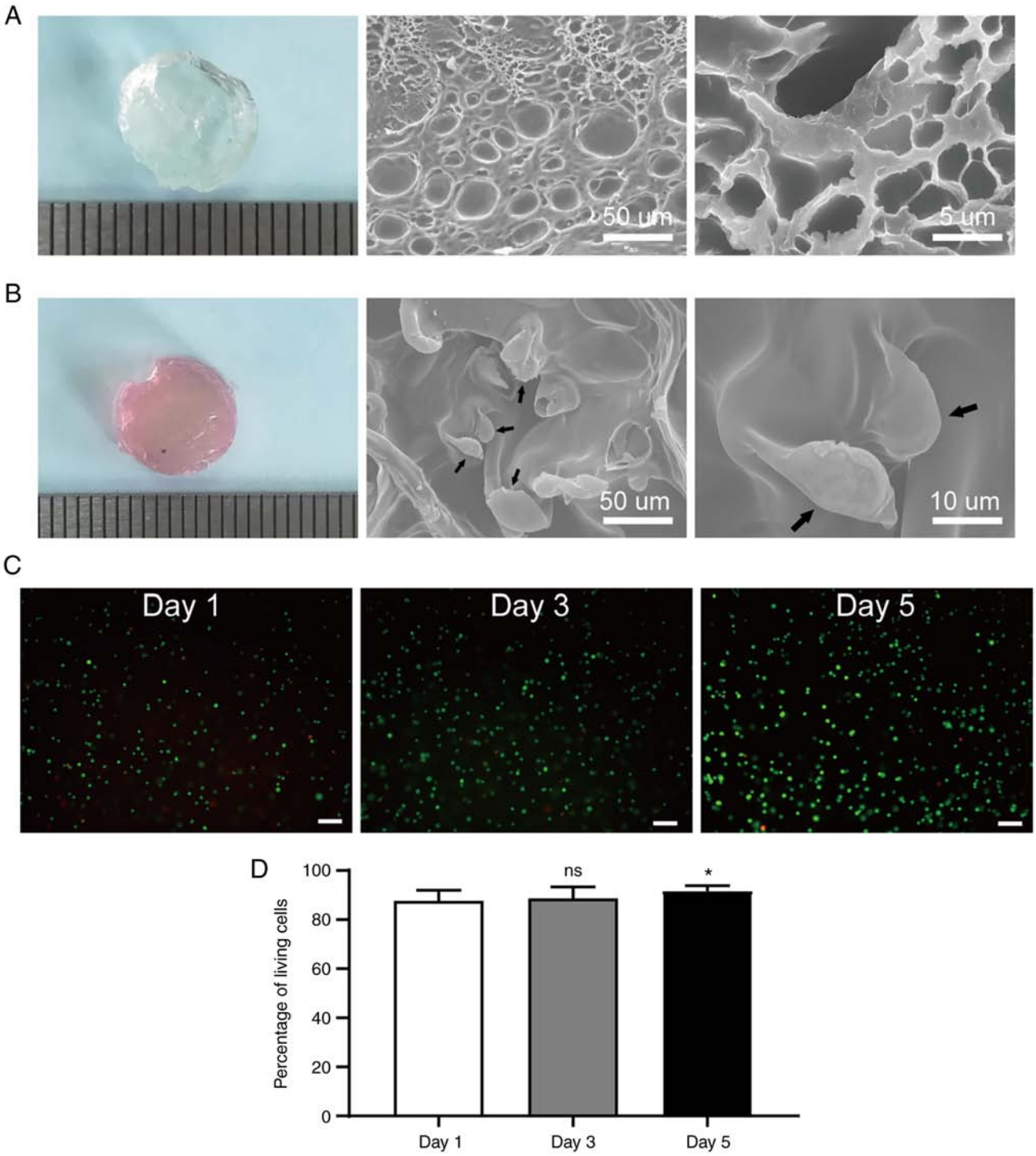

Figure 2. Characterization of GelMA hydrogel. (A) Appearance (left panel) and SEM images (right panel) of the GelMA hydrogel. (B) Appearance (left panel) and SEM images (right panel) of the ASC-laden GelMA hydrogel. Arrows indicate Schwann cells encapsulated in the GelMA hydrogel. (C) Representative immunofluorescence images of co-culture cells encapsulated in the GelMA hydrogel. Green (Calcein AM) and red (PI) fluorescence indicate live cells and dead cells, respectively. Scale bars, 100 μm. (D) Quantification of the percentage of alive ASCs encapsulated in the GelMA hydrogel on days 1, 3 and 5. The data shown are the mean ± standard deviation (n=6 in each group). *P<0.05 compared with day 1. GelMA, gelatin methacryloyl; SEM, scanning electron microscopy; ASCs, activated Schwann cells; ns, not significant.

Transplantation of GelMA/ASCs inhibits cell apoptosis following SCI. To investigate cell apoptosis, TUNEL staining and Bcl-2 immunochemistry were performed on the 7th day. For TUNEL staining, compared with the sham group, the number of apoptotic cells in the SCI group was increased (Fig. 5A). The ASC (P<0.01) and GelMA/ASC (P<0.001) groups both exhibited a significantly decreased number of apoptotic cells compared with the SCI group, and GelMA/ASC treatment was found to be more advantageous as compared with single ASC treatment in inhibiting cell apoptosis (P<0.05) (Fig. 5C).

The Bcl-2 positive cells exhibited a brown-stained cytoplasm. In the sham group, a great number of Bcl-2 positive cells appeared, while in the SCI group, only a small number of cells were Bcl-2-immunoreactive (Fig. 5B). In the ASC group,

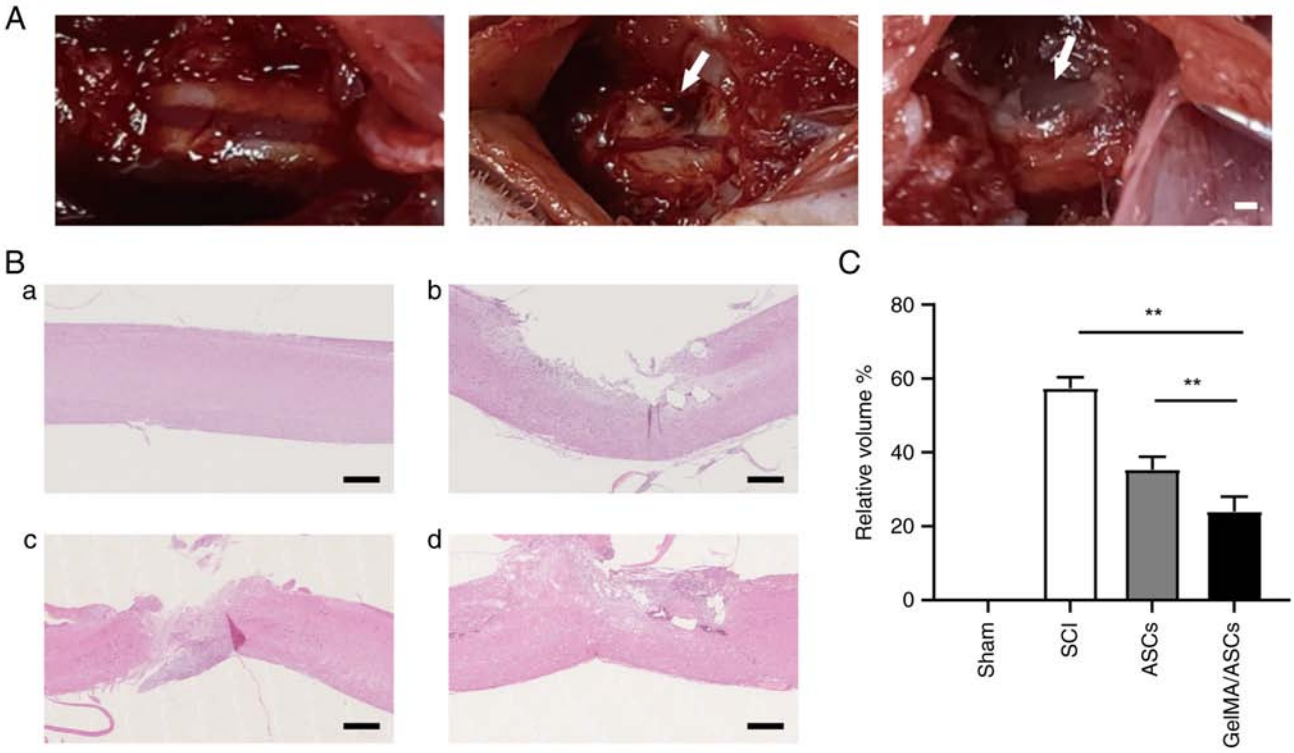

Figure 3. GelMA hydrogel loaded with ASCs reduces lesion volume in rats following SCI. (A) Spinal cord hemi-transection and scaffold transplantation. Scale bar, 0.1 cm. (B) Representative sagittal images of hematoxylin and eosin staining of spinal cord tissues in the (a) sham group, (b) SCI group, (c) ASC treatment group, and (d) GelMA/ASCs transplantation group after 6 weeks of treatment. Scale bar, 200 μm. (C) Quantification of the cavity volume as a percentage of the volume of the lesion lumen in each group. Arrows indicate the lesion site before and after gel transplantation. The data shown are the mean ± standard deviation (n=6 in each group). **P<0.01 compared with the SCI group. GelMA, gelatin methacryloyl; SCI, spinal cord injury; ASCs, activated Schwann cells.

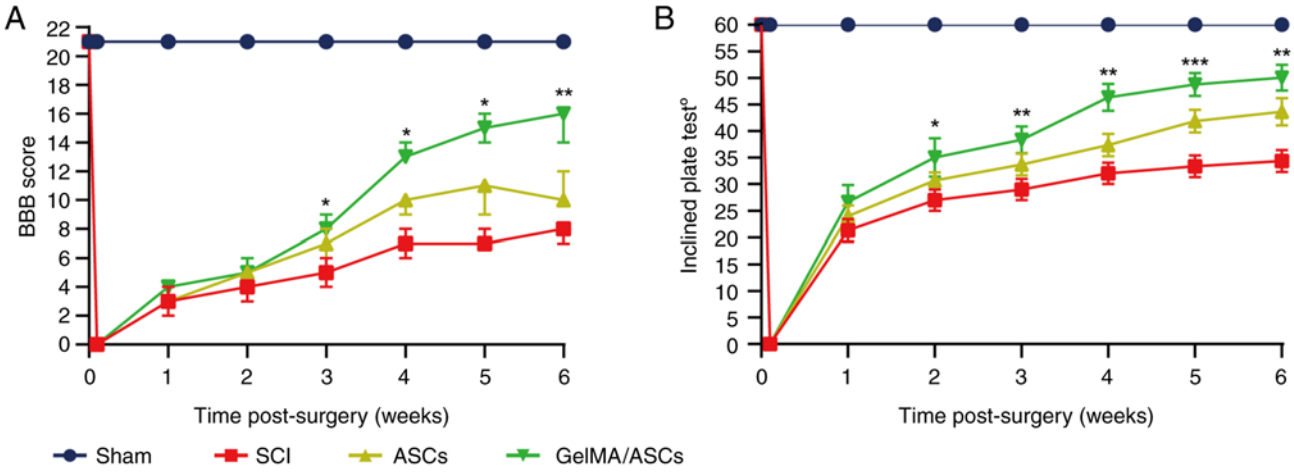

Figure 4. GelMA/ASC implants promote motor functional recovery in rats following SCI. (A) BBB scoring system was applied for hindlimb locomotion assessment from weeks 1 to 6 post-surgery. (B) The inclined test was performed from weeks 1 to 6 post-surgery. The data shown are the median (IQR) and mean ± standard deviation for BBB score and inclined test, respectively (n=12 in each group). *P<0.05, **P<0.01 and ***P<0.001 compared with the SCI group. GelMA, gelatin methacryloyl; ASCs, activated Schwann cells; SCI, spinal cord injury; BBB, Basso-Beattie-Bresnahan; IQR, interquartile range.

there were more Bcl-2-positive cells than SCI group (P<0.01); however, this number was lower than that in the GelMA/ASC group (P<0.05) (Fig. 5D).

p38 MAPK is involved in the decreased cell apoptosis following transplantation treatment. The levels of apoptosis-related proteins, caspase-3 and Bcl-2, were further verified using western blot analysis. The results of quantitative analysis demonstrated that, following SCI, the expression of the pro-apoptotic protein, caspase-3, significantly increased (P<0.01), indicating a higher rate of cell death, while GelMA/ASC transplantation decreased the protein level of caspase-3 (P<0.05). The expression of the anti-apoptotic protein, Bcl-2, was consistent with the results of immunochemistry. Compared with the SCI group, the protein expression of Bcl-2 in the ASC (P<0.05) and

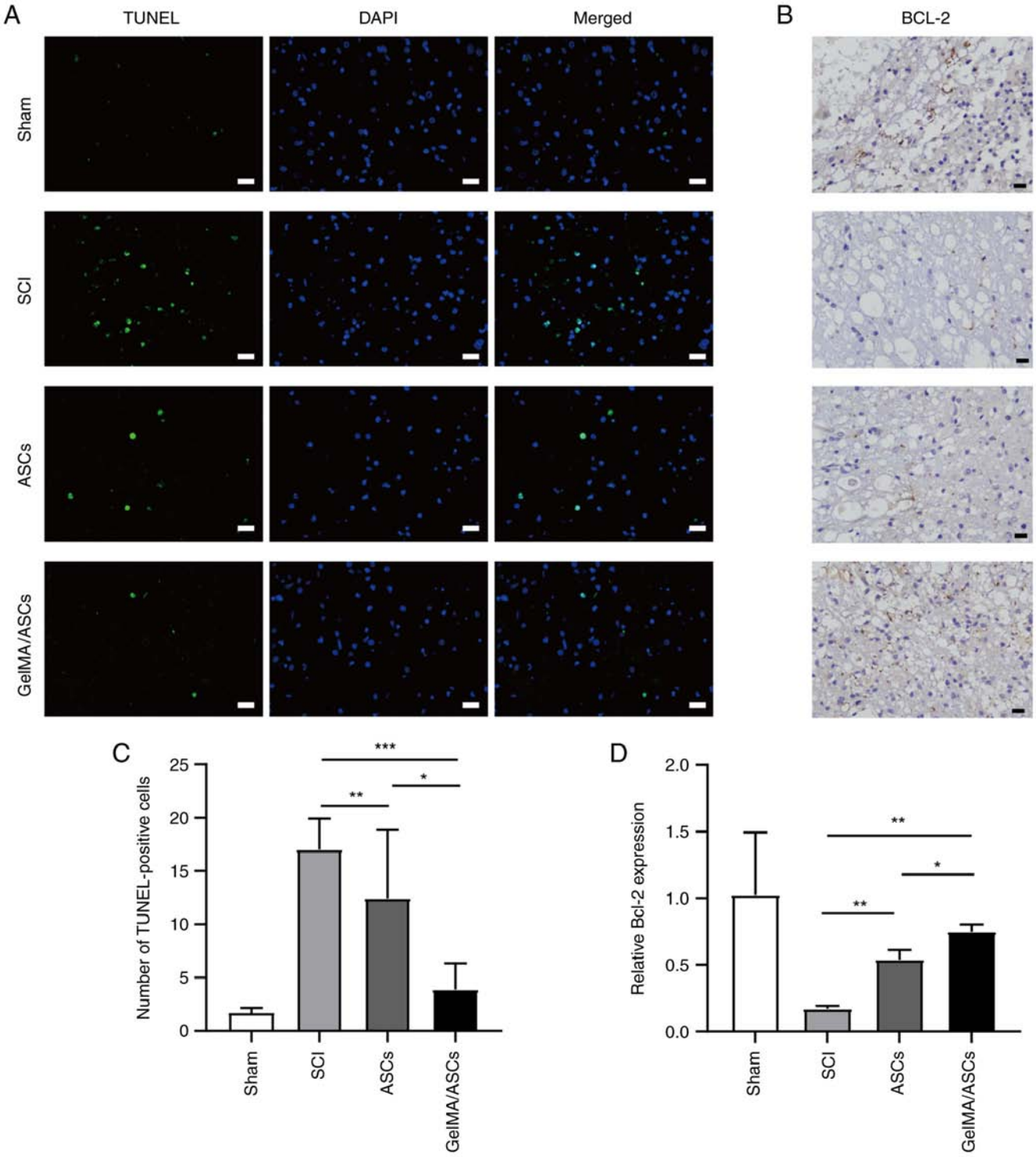

Figure 5. Cell apoptosis is detected using TUNEL staining and Bcl-2 immunochemistry. (A) Representative immunofluorescence images of TUNEL staining in each group on day 7 post-surgery. Scale bar, 25 μm. (B) Representative photomicrographs of Bcl-2 immunochemistry in each group on day 7 post-surgery. Scale bar, 25 μm. (C) Quantification of TUNEL-positive cells. (D) Quantification of the relative expression of Bcl-2 gene. The data shown are the mean ± standard deviation (n=6 in each group). *P<0.05, **P<0.01 and ***P<0.001 compared with the SCI or ASC group. ASCs, activated Schwann cells; SCI, spinal cord injury.

GelMA/ASC group (P<0.01) was significantly increased (Fig. 6A and B).

To examine the mechanisms of GelMA/ASCs in inhibiting cell apoptosis following SCI, three important components of the MAPK family were detected, including p38, ERK1/2 and JNK1/2. It was found that the activity of the MAPK family was activated following SCI compared with that of the sham group (p38: P<0.01; ERK1/2 and JNK1/2: P<0.05) (Fig. 6C and D). However, transplantation treatment decreased the phosphorylation level of p38 signaling (ASCs: P<0.05; GelMA/ASCs: P<0.01), while that of ERK1/2 and JNK1/2 signaling were relatively unaltered (Fig. 6C and D). Collectively, the results

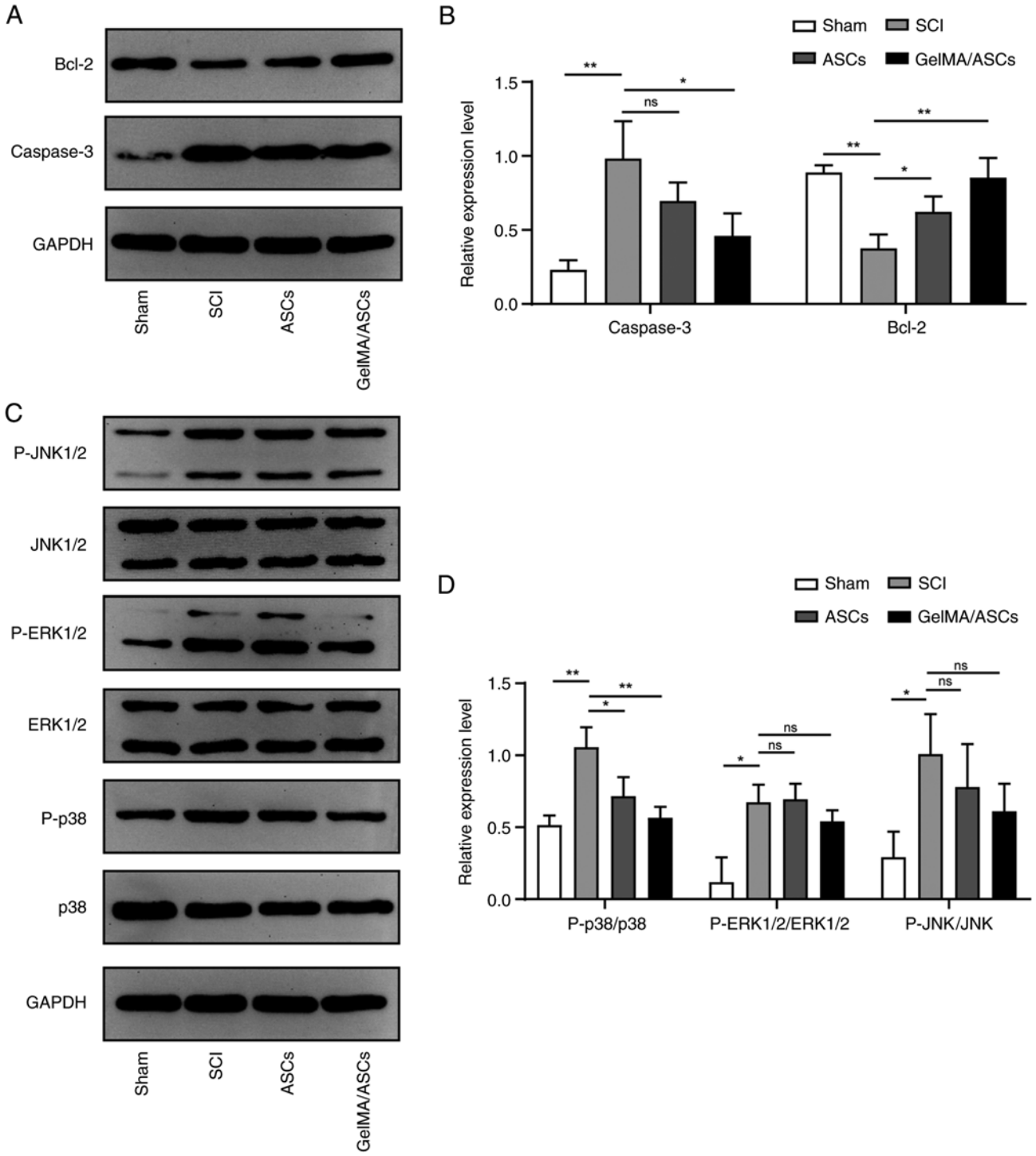

Figure 6. Apoptosis-related proteins and pathways detected using western blot analysis. (A and B) Representative western blots and quantification of expression levels for protein caspase-3 and Bcl-2 in each group at 7 days post-surgery. (C and D) Detection of apoptosis-related pathways, including p38, ERK1/2, and JNK1/2. The data shown are the mean ± standard deviation (n=6 in each group). *P<0.05 and **P<0.01 compared with the SCI or ASC group. ASCs, activated Schwann cells; SCI, spinal cord injury; ns, no significance.

indicated that GelMA/ASC treatment decreased cell apoptosis following SCI and that these effects may be mediated via the p38 MAPK pathway.

Discussion

Numerous studies have confirmed the effectiveness of SC transplantation in the treatment of SCI. However, SCs are known for having two different states and the majority of studies have focused on their normal states (NSCs). Studies on the transplantation of ASCs in the treatment of SCI are limited. Compared with NSCs, ASCs have a higher cell proliferative and adhesive ability, and can synthesize and secrete various neurotrophic factors (25). Marcol *et al* (26) used ASCs to repair focal injury in the spinal cords of rats. In particular, they found the transplanted ASCs could elicit the body's self-repair

by inducing endogenous SCs in the nerve root to migrate to the lesion site (26). Moreover, a previous study by the authors demonstrated that the clinical application of ASCs in the treatment of patients with SCI exhibited promising prospects (15). The present study successfully isolated ASCs, as previously described, and used them to repair the hemisection injury in the spinal cord of rats. It was found that ASC treatment attenuated cell apoptosis, rebuilt the disordered structure of the injured spinal cord, and further improved the functional recovery of rats with SCI. The present study highlights the feasibility of using ASCs in the treatment of SCI.

Currently, the use of biological material is making progress in regenerative medicine. A favorable biomaterial should be biocompatible and biodegradable with a low immunogenicity and GelMA hydrogel possesses these properties (27,28). Moreover, the inner 3D structure and tunable mechanistic characteristics of the GelMA hydrogel render it effective in various tissue repair regions (spinal cord, bone and cardio) (29). The present study constructed an ASC-GelMA hydrogel composite. The results of SEM and live/dead staining revealed that the ASCs survived and proliferated in the GelMA hydrogel. The locomotor test and H&E staining revealed that the GelMA/ASCs repaired the injured spinal cord and enhanced functional recovery. Moreover, the post-operative recovery in the GelMA/ASC group was improved compared with that in the ASC group, which suggests that the GelMA hydrogel may enhance the therapeutic efficacy of single ASC treatment. Overall, these findings indicated that the GelMA/ASC implant is a promising therapeutic strategy for SCI.

Cell apoptosis is a very common phenomenon following SCI. It occurs when cells survive from initial trauma, yet endure sufficient insult, which activates relevant apoptotic pathways. Generally, in rat SCI, cell apoptosis occurs as early as 4 h following SCI and peaks on the 7th day (30,31). In the present study, to examine the anti-apoptotic effects of ASCs and GelMA/ASCs, the injured spinal cord was collected on the 7th day following SCI and TUNEL staining was performed. Compared with the SCI group, the number of TUNEL-positive cells in the treatment group (the ASC and GelMA/ASC groups) decreased significantly. Neural survival is the prerequisite of neural regeneration. Thus, these results may explain why the lesion areas in the treatment group were reduced. Moreover, the numbers of TUNEL-positive cells in the GelMA/ASC group were lower than those in the ASC group which may be attributed to the beneficial effects of the GelMA hydrogel on the ASCs and injured spinal cord. Furthermore, the Bcl-2 gene has an anti-apoptotic effect and its overexpression can inhibit the occurrence of cell apoptosis (32,33). In the present study, the results of immunochemistry revealed similar trends as those observed with TUNEL staining. On the whole, ASCs and GelMA/ASCs may alleviate SCI by attenuating cell apoptosis.

MAPK is a type of serine/threonine protein kinase that plays crucial roles in signal transduction from the cell surface to the nucleus, thereby regulating cell fate (proliferation, apoptosis and differentiation) (34,35). There are three important members in the MAPK family, including p38, ERK1/2 and JNK1/2 and they are known to mediate various cellular responses in the form of phosphorylation (36). It has been well documented that the activation of the MAPK pathway is involved in the inflammatory response, gliosis and apoptosis following SCI (37,38). In the present study, the protein expression of the MAPK family was significantly increased following SCI, which is consistent with the findings of a previous study (24). However, transplantation treatment could not inhibit the activation of ERK1/2 and JNK1/2 signaling, while the protein expression of p38 was significantly decreased. Previous research has demonstrated that p38 MAPK exerts a growth inhibitory effect (39). Thus, the findings of the present study indicated that GelMA/ASC implants can inhibit p38 MAPK pathway activation to reduce cell apoptosis, thereby protecting the injured spinal cord.

In the present study, ASCs and GelMA hydrogel were utilized to create a tissue engineering scaffold. The cell-containing scaffold displayed favorable biocompatibility and inhibited cell apoptosis, promoting tissue remolding following transplantation *in vivo*. Furthermore, this tissue engineering scaffold promoted motor functional recovery in rats with SCI. The present study demonstrated that GelMA/ASC scaffolds may prove to be a clinically effective strategy for the treatment of SCI in the future. However, several limitations in the present study need to be acknowledged. Firstly, the present study did not perform experiments to analyze the comparison between NSCs and ASCs; however, relevant results were included in previously published studies (22). Secondly, the therapeutic efficacy of GelMA/ASCs scaffolds was not further verified in some larger mammals and the images or videos of rat's behavior tests were also not recorded timely in this study. Lastly, certain other pathophysiology changes following SCI, such as inflammation, angiogenesis and remyelination need to be further elucidated. Therefore, in the future, the authors aim to focus on the underlying mechanisms of GelMA/ASCs in the treatment of SCI and to further verify the therapeutic efficacy of GelMA/ASCs in animal models of SCI using larger mammals.

Acknowledgements

Not applicable.

Funding

The present study was supported by grants from the National Natural Science Foundation of China (grant nos. 81972061, 81871766 and 81902216).

Availability of data and materials

The datasets used and/or analyzed during the current study are available from the corresponding author on reasonable request.

Authors' contributions

YL and HY contributed to the study design and data analysis. HY wrote the manuscript. YL and PY performed the majority of the experiments. PP, CL and ZX assisted with experiments, data analysis and interpretation as well as contributing to the critical revision of the manuscript for intellectual content. DB made substantial contributions to conception and design as well as giving final approval of the version to be published. HY, YL and PY were equal contributors to the study. YL and DB confirm the authenticity of all the raw data. All authors have read and approved the final manuscript.

Ethics approval and consent to participate

The present study was approved (approval no. MDL20210810-01) by the Ethics Committee of The Tianjin Medical University General Hospital (Tianjin, China).

Patient consent for publication

Not applicable.

Competing interests

The authors declare that they have no competing interests.

References

1. Ahuja CS, Wilson JR, Nori S, Kotter MRN, Druschel C, Curt A and Fehlings MG: Traumatic spinal cord injury. Nat Rev Dis Primers 3: 17018, 2017.
2. Fan B, Wei Z, Yao X, Shi G, Cheng X, Zhou X, Zhou H, Ning G, Kong X and Feng S: Microenvironment imbalance of spinal cord injury. Cell Transplant 27: 853-866, 2018.
3. Ahuja CS, Nori S, Tetreault L, Wilson J, Kwon B, Harrop J, Choi D and Fehlings MG: Traumatic spinal cord injury-repair and regeneration. Neurosurgery 80 (3S): S9-S22, 2017.
4. Courtine G and Sofroniew MV: Spinal cord repair: Advances in biology and technology. Nat Med 25: 898-908, 2019.
5. Assinck P, Duncan GJ, Hilton BJ, Plemel JR and Tetzlaff W: Cell transplantation therapy for spinal cord injury. Nat Neurosci 20: 637-647, 2017.
6. Zhou P, Guan J, Xu P, Zhao J, Zhang C, Zhang B, Mao Y and Cui W: Cell therapeutic strategies for spinal cord injury. Adv Wound Care (New Rochelle) 8: 585-605, 2019.
7. Piltti KM, Funes GM, Avakian SN, Salibian AA, Huang KI, Carta K, Kamei N, Flanagan LA, Monuki ES, Uchida N, *et al*: Increasing human neural stem cell transplantation dose alters oligodendroglial and neuronal differentiation after spinal cord injury. Stem Cell Reports 8: 1534-1548, 2017.
8. Nicaise AM, Banda E, Guzzo RM, Russomanno K, Castro-Borrero W, Willis CM, Johnson KM, Lo AC and Crocker SJ: iPS-derived neural progenitor cells from PPMS patients reveal defect in myelin injury response. Exp Neurol 288: 114-121, 2017.
9. Liu S, Schackel T, Weidner N and Puttagunta R: Biomaterial-Supported cell transplantation treatments for spinal cord injury: Challenges and perspectives. Front Cell Neurosci 11: 430, 2018.
10. Marquardt LM, Doulames VM, Wang AT, Dubbin K, Suhar RA, Kratochvil MJ, Medress ZA, Plant GW and Heilshorn SC: Designer, injectable gels to prevent transplanted Schwann cell loss during spinal cord injury therapy. Sci Adv 6: eaaz1039, 2020.
11. Assunção-Silva RC, Gomes ED, Sousa N, Silva NA and Salgado AJ: Hydrogels and cell based therapies in spinal cord injury regeneration. Stem Cells Int 2015: 948040, 2015.
12. Jessen KR, Mirsky R and Lloyd AC: Schwann cells: Development and role in nerve repair. Cold Spring Harb Perspect Biol 7: a020487, 2015.
13. Feltri ML, Poitelon Y and Previtali SC: How Schwann cells sort axons: New concepts. Neuroscientist 22: 252-265, 2016.
14. Hill CE, Moon LD, Wood PM and Bunge MB: Labeled Schwann cell transplantation: Cell loss, host Schwann cell replacement, and strategies to enhance survival. Glia 53: 338-343, 2006.
15. Zhou XH, Ning GZ, Feng SQ, Kong XH, Chen JT, Zheng YF, Ban DX, Liu T, Li H and Wang P: Transplantation of autologous activated Schwann cells in the treatment of spinal cord injury: Six cases, more than five years of follow-up. Cell Transplant 21 (Suppl 1): S39-S47, 2012.
16. Monje PV, Deng L and Xu XM: Human Schwann cell transplantation for spinal cord injury: Prospects and challenges in translational medicine. Front Cell Neurosci 15: 690894, 2021.
17. Yue K, Trujillo-de Santiago G, Alvarez MM, Tamayol A, Annabi N and Khademhosseini A: Synthesis, properties, and biomedical applications of gelatin methacryloyl (GelMA) hydrogels. Biomaterials 73: 254-271, 2015.
18. Khayat A, Monteiro N, Smith EE, Pagni S, Zhang W, Khademhosseini A and Yelick PC: GelMA-encapsulated hDPSCs and HUVECs for dental pulp regeneration. J Dent Res 96: 192-199, 2017.
19. Nichol JW, Koshy S, Bae H, Hwang CM, Yamanlar S and Khademhosseini A: Cell-laden microengineered gelatin methacrylate hydrogels. Biomaterials 31: 5536-5544, 2010.
20. Fan L, Liu C, Chen X, Zou Y, Zhou Z, Lin C, Tan G, Zhou L, Ning C and Wang Q: Directing induced pluripotent stem cell derived neural stem cell fate with a three-dimensional biomimetic hydrogel for spinal cord injury repair. ACS Appl Mater Interfaces 10: 17742-17755, 2018.
21. Zhou P, Xu P, Guan J, Zhang C, Chang J, Yang F, Xiao H, Sun H, Zhang Z, Wang M, *et al*: Promoting 3D neuronal differentiation in hydrogel for spinal cord regeneration. Colloids Surf B Biointerfaces 194: 111214, 2020.
22. Shi GD, Cheng X, Zhou XH, Fan BY, Ren YM, Lin W, Zhang XL, Liu S, Hao Y, Wei ZJ and Feng SQ: iTRAQ-based proteomics profiling of Schwann cells before and after peripheral nerve injury. Iran J Basic Med Sci 21: 832-841, 2018.
23. Basso DM, Beattie MS and Bresnahan JC: A sensitive and reliable locomotor rating scale for open field testing in rats. J Neurotrauma 12: 1-21, 1995.
24. Duan HQ, Wu QL, Yao X, Fan BY, Shi HY, Zhao CX, Zhang Y, Li B, Sun C, Kong XH, *et al*: Nafamostat mesilate attenuates inflammation and apoptosis and promotes locomotor recovery after spinal cord injury. CNS Neurosci Ther 24: 429-438, 2018.
25. Zhou XH, Lin W, Ren YM, Liu S, Fan BY, Wei ZJ, Shi GD, Cheng X, Hao Y and Feng SQ: Comparison of DNA methylation in Schwann cells before and after peripheral nerve injury in rats. Biomed Res Int 2017: 5393268, 2017.
26. Marcol W, Ślusarczyk W, Larysz-Brysz M, Francuz T, Jędrzejowska-Szypułka H, Łabuzek K and Lewin-Kowalik J: Grafted activated Schwann cells support survival of injured rat spinal cord white matter. World Neurosurg 84: 511-519, 2015.
27. Katoh H, Yokota K and Fehlings MG: Regeneration of spinal cord connectivity through stem cell transplantation and biomaterial scaffolds. Front Cell Neurosci 13: 248, 2019.
28. Malikmammadov E, Tanir TE, Kiziltay A, Hasirci V and Hasirci N: PCL and PCL-based materials in biomedical applications. J Biomater Sci Polym Ed 29: 863-893, 2018.
29. Xiao S, Zhao T, Wang J, Wang C, Du J, Ying L, Lin J, Zhang C, Hu W, Wang L and Xu K: Gelatin methacrylate (GelMA)-based hydrogels for cell transplantation: An effective strategy for tissue engineering. Stem Cell Rev Rep 15: 664-679, 2019.
30. Li GL, Farooque M and Olsson Y: Changes of Fas and Fas ligand immunoreactivity after compression trauma to rat spinal cord. Acta Neuropathol 100: 75-81, 2000.
31. Park E, Liu Y and Fehlings MG: Changes in glial cell white matter AMPA receptor expression after spinal cord injury and relationship to apoptotic cell death. Exp Neurol 182: 35-48, 2003.
32. Chen DF and Tonegawa S: Why do mature CNS neurons of mammals fail to re-establish connections following injury-functions of bcl-2. Cell Death Differ 5: 816-822, 1998.
33. Wang C, Zhang L, Ndong JC, Hettinghouse A, Sun G, Chen C, Zhang C, Liu R and Liu CJ: Progranulin deficiency exacerbates spinal cord injury by promoting neuroinflammation and cell apoptosis in mice. J Neuroinflammation 16: 238, 2019.
34. Crown ED, Gwak YS, Ye Z, Johnson KM and Hulsebosch CE: Activation of p38 MAP kinase is involved in central neuropathic pain following spinal cord injury. Exp Neurol 213: 257-267, 2008.
35. Kasuya Y, Umezawa H and Hatano M: Stress-activated protein kinases in spinal cord injury: Focus on roles of p38. Int J Mol Sci 19: 867, 2018.
36. Zhan J, He J, Chen M, Luo D and Lin D: Fasudil promotes BMSC migration via activating the MAPK signaling pathway and application in a model of spinal cord injury. Stem Cells Int 2018: 9793845, 2018.
37. Chen NN, Wei F, Wang L, Cui S, Wan Y and Liu S: Tumor necrosis factor alpha induces neural stem cell apoptosis through activating p38 MAPK pathway. Neurochem Res 41: 3052-3062, 2016.
38. Qian Z, Chang J, Jiang F, Ge D, Yang L, Li Y, Chen H and Cao X: Excess administration of miR-340-5p ameliorates spinal cord injury-induced neuroinflammation and apoptosis by modulating the P38-MAPK signaling pathway. Brain Behav Immun 87: 531-542, 2020.
39. Zhu J, Yu W, Liu B, Wang Y, Shao J, Wang J, Xia K, Liang C, Fang W, Zhou C and Tao H: Escin induces caspase-dependent apoptosis and autophagy through the ROS/p38 MAPK signalling pathway in human osteosarcoma cells in vitro and in vivo. Cell Death Dis 8: e3113, 2017.